Journal of chemical & engineering data

Article

pubs.acs.org/jced

Molecular Dynamics Study of the Local Structure of Photovoltaic Polymer PCDTBT

Yusuke Kawanabe, Adam J. Moulé, and Roland Faller*

Department of Chemical Engineering and Materials Science, University of California, Davis, California 95616, United States

ABSTRACT: To meet the huge demand for renewable energy, significant research effort focuses on creating efficient organic photovoltaic (OPV) devices. In comparison to silicon-based semiconductors, OPV materials have many superior properties such as cost effectiveness, being lightweight, and flexibility, which lead to a high potential for the replacement of silicon-based semiconductors. Recently, a large number of new alternating copolymer materials have demonstrated high power conversion efficiency (PCE). These successful polymers typically have low long-range order but a high hole mobility which directly affects the PCE which depends on polymer structure. In this study, a solution molecular model for poly[*N*-9″-hepta-decanyl-2,7-carbazole-*alt*-5,5-(4′,7′-di-2-thienyl-2′,1′,3′-benzothiadiazole)]:[6,6]-phenyl (PCDTBT) is developed and subsequently a molecular dynamics simulation conducted in order to understand the structure of the polymer solution. The simulation results are consistent with a low-solubility polymer that requires long equilibration times to planarize. The structural addition of side chains to inhibit rotation of thiophene rings could improve the conjugation and processability of PDCTBT leading to further improvements in OPV efficiency or hole mobility.

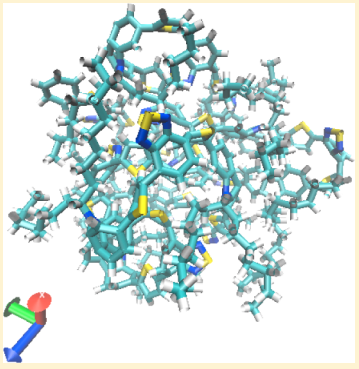

I. INTRODUCTION

Organic photovoltaic (OPV) devices are a product of a blooming cost-efficient technology, which can potentially replace silicon-based photovoltaic cells.[1] OPV devices have many advantages: affordability, solution processability and flexibility along with being lightweight and having low environmental impact. However, they have a lower power conversion efficiency (PCE) compared to conventional photovoltaic systems. The highest reported PCE of an OPV cell is just over 12%[2] for a two junction device. The electron generation in the 12% record device occurs at a bilayer donor/acceptor heterojunction.[2,3] Most OPV devices are fabricated from a mixture of donor and acceptor materials in a so-called bulk heterojunction (BHJ) device.[4] BHJ technology has enabled the development of single junction OPV devices with a PCE of 9.2%.[5]

It is important to choose efficient materials for OPV devices. Poly[*N*-9″-hepta-decanyl-2,7-carbazole-*alt*-5,5-(4′,7′-di-2-thienyl-2′,1′,3′-benzothiadiazole)]:[6,6]-phenyl (PCDTBT) is one of the most efficient donors, and its highest PCE is reported to be 6.5% in a 110 nm thick layer.[5,6] The high PCE, comes from favorable properties including a low band gap (1.8 eV), a high ionization energy (increases the open circuit voltage), and a high hole mobility (μ_h) that is required in order to effectively remove photoexcited holes from the heterojunction layer.[7] A large number of studies link polymer morphology and processing conditions to the formation of traps in OPV devices, but more detailed studies of the atomistic structure of PCDTBT are necessary to determine the structural origin of these traps.[7−22] It is known that PCDTBT has low solubility in all solvents, which makes the study of structure and trap sites more difficult.

We present the first molecular simulation model of PCDTBT and examine the dynamics and molecular conformations of PCDTBT using atomistic molecular dynamics (MD) of the polymer in solution as a first step to develop more complex device relevant studies in the future. MD simulations can determine structure and conformations as indicators of the efficiency of organic semiconductors.[23,24] We can therefore get indications on the hole mobility as this largely depends on the conformation of a polymer.

We developed an atomistic computer model of PCDTBT in toluene (Figure 1) to examine the configurations of the

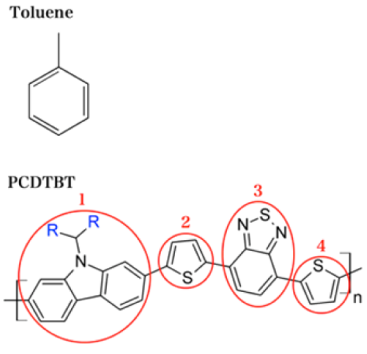

Figure 1. Chemical structure of toluene and PCDTBT. The sites used for dihedral analysis are labeled.

Special Issue: Modeling and Simulation of Real Systems

Received: January 28, 2014
Accepted: September 5, 2014
Published: September 9, 2014

polymer to gain initial insight into structure−property relationships of materials for OPVs. In particular, to achieve a high hole mobility (μ_h), one needs overlap of π orbitals along the chain such that carriers (holes) can move easily along the backbone. To create this overlap, the polymer backbone configuration has to be straight and planar to avoid breaking conjugation.

II. COMPUTATIONAL METHODS

Molecular dynamics (MD) simulations were carried out with GROMACS 4.5[25] for a 12-mer of PCDTBT in toluene. Some simulations also were performed using 4 12-mers. The general Amber Force Field (GAFF) was used.[26,27] We used Antechamber to assign force field parameters and electric charges using Austin Model 1 calculations in MOPAC.[28]

The polymer was placed into a cubic box of 6 × 6 x 6 nm^3 filled with toluene at a density of 0.855 g/mL avoiding overlaps. After initial energy minimization (EM) the temperature was gradually increased from 200 K to 300 K using MD. After equilibration an MD simulation was performed in the *NPT* ensemble (constant number of molecules, *N*; pressure, *P*; and temperature, *T*), using the Nose−Hoover thermostat and the Parrinello−Rahman barostat with coupling times of τ_T = 0.15 ps and τ_P = 0.15 ps and a cutoff of 1.4 nm both for the Lennard-Jones and for the reaction field electrostatics (ε = 78). Fourth order interpolation and periodic boundary conditions for all dimensions were used. The simulation was carried out for 8 ns with a time step of 1.4 fs at ambient temperature (298 K) and atmospheric pressure (101.3 kPa). The simulation with four polymers was run for 3 ns. Figures 2 to 4 show visualizations of the system with and without solvent. It is obvious that the polymer is very weakly soluble and single chains do not stretch out to minimize solvent contact. In the simulation with multiple chains we see weak aggregation of the chains.

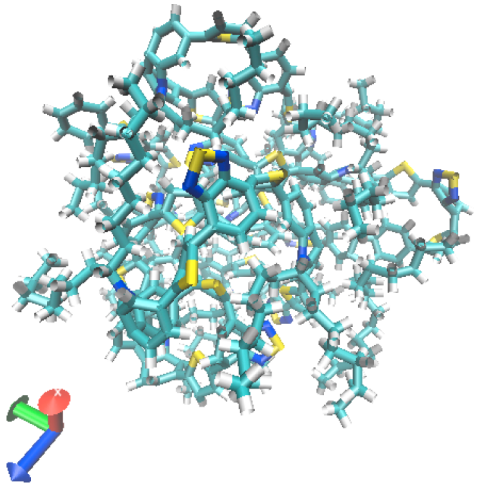

Figure 2. Visualization of PCDTBT 12-mer after energy minimization.

III. RESULTS AND DISCUSSION

Important general characteristics of the polymers in the single chain simulations are calculated in order to reveal the configurations of the polymer in solution. First, the radius of gyration is obtained. The radius of gyration for each direction is shown in Table 1 and varies in the range of 0.85 nm to 1.2 nm.

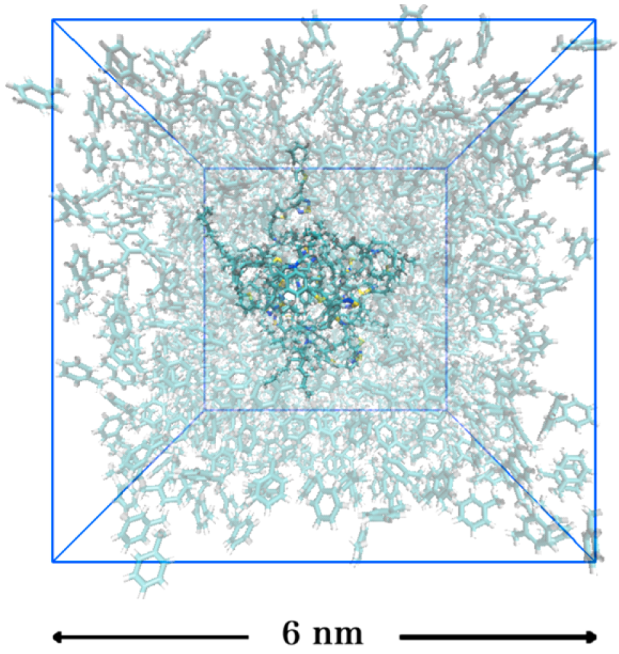

Figure 3. Configuration from an MD simulation of one PCDTBT 12-mer in a box with 945 toluenes.

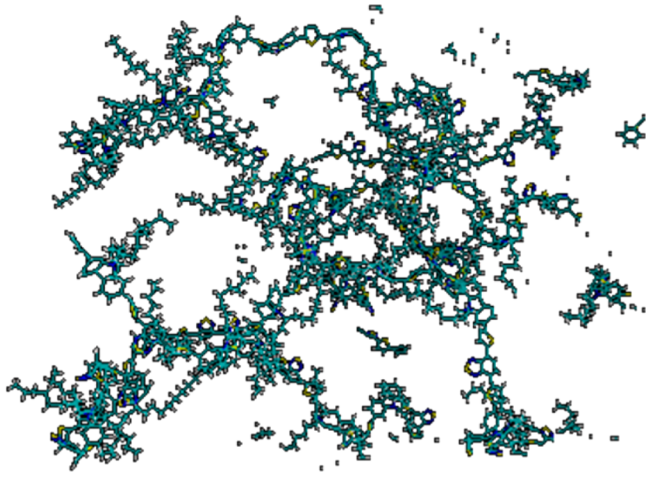

Figure 4. Configuration from an MD simulation of four PCDTBT 12-mer in a box with 2388 toluenes (solvent not shown).

Table 1. Average Radius of Gyration of Solute PCDTBT for Each Direction

	radius of gyration
x	(1.005 ± 0.002) nm
y	(1.004 ± 0.002) nm
z	(1.030 ± 0.002) nm

The polymer is rather compact and on average spherical (cf. Figure 2). Random coil polymers in contrast have normally an ellipsoidal shape. Second, we measured the short time (3 ns < *t* < 5 ns) mean squared displacement of both the polymer and toluene for their centers of mass (Figure 5). Short-term diffusion coefficients using the Einstein relation are shown in Table 2. This data indicates equilibration of the structure.

A planar configuration leads to high hole mobility of the polymer because the formation of π orbitals enhances hole movement and the rotated structure between two cyclic

dx.doi.org/10.1021/je500101b | J. Chem. Eng. Data 2014, 59, 2982−2986

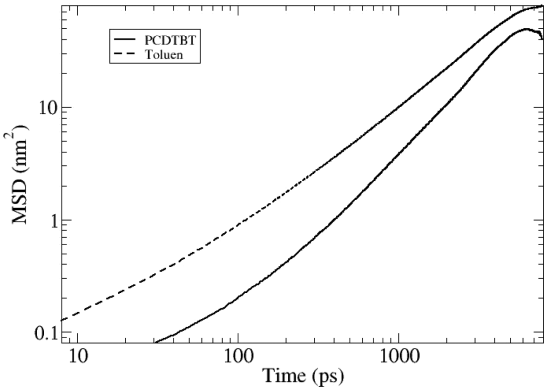

Figure 5. Mean square displacement of PCDTBT and toluene center of mass in a log−log plot through out the simulation time range.

Table 2. Average Short Diffusion Coefficient of Solute PCDTBT and Solvent Toluene Throughout Simulation

	diffusion coefficient
PCDTBT	1.84×10^{-9} m^2/s ± 3.46×10
toluene	2.20×10^{-9} m^2/s ± 4.25×10^{-3}

aromatic compounds leads to less electronic overlap due to misalignment.[29] However, a planar configuration of the dihedral bonds also leads to low solubility. Experimentally this polymer has a rather high hole mobility and low solubility, indicating conjugation over a number of rings. To examine this overlap in solution, we measured the dihedral angle between segments 1, 2, 3, and 4 (defined in Figure 1). The result of dihedral analysis is shown in Figure 6, where dihedral angles of 0° and 180°

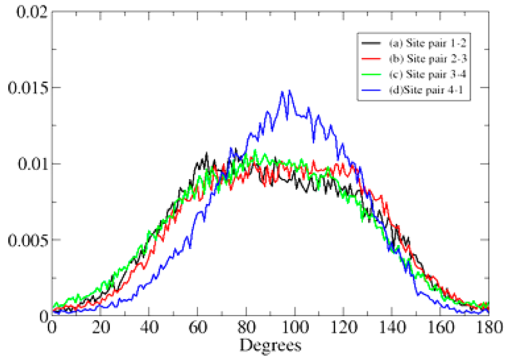

Figure 6. Dihedral distribution for site pair (a) 1−2, (b) 2−3, (c) 3−4, and (d) 4−1 at 1 bar, 300 K.

indicate planar configurations. All distributions of dihedral angles show peaks around 100° but they vary in a wide range of 50° to 130°. It might be assumed that the reason why all dihedrals have peaks around 90° to 100° is an unbalanced electron distribution caused by the sulfur on the thiophene rings. Those electron-rich sites repel each other and the dihedral angles average around 90°. Because of similar structure dihedrals 2−3 and pair 3−4 have similar distribution. Because of the rotational freedom along the backbone of this polymer, the dihedrals have large variations in solution. We have not modeled PCDTBT in a melt, but can speculate that the large dihedral distribution in solution will lead to long equilibration times for solution cast samples, which is seen experimentally. The wide dihedral angle distribution in solution also suggests that the planar (all conjugated) polymer structure that is desired in an OPV device for high μ_h is not favored thermodynamically for low concentration in solution. However, multichain interactions like ring stacking might lead to much better planarity in melt or solid phases. Also as this polymer is only weakly soluble, we find bundles of more than one chain in solution, as seen in Figure 4, where better conjugation would be expected as well.

Radial distribution of the solvent with respect to the monomer determines solvent quality and is given in Figure 7

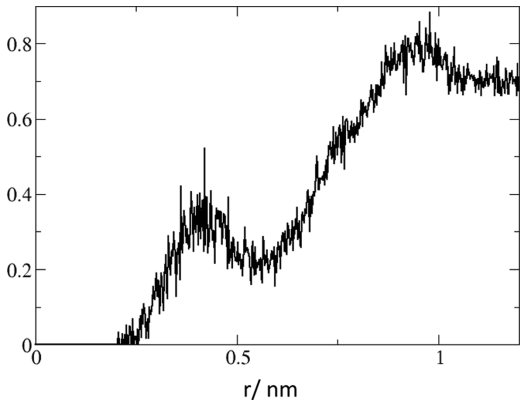

Figure 7. Radial distribution function (RDF) of the centers-of-mass of the monomers to the centers-of-mass of toluene as a function of distance.

for the single chain simulations. The distribution has a shoulder at 0.5 nm and a peak at 0.9 nm. We also see the clear polymer correlation hole. This gives us the insight into the distribution of solvent around the polymer that solvent can get as close as about 0.5 nm to the polymer, but the major first shell is at 0.9 nm. Therefore, those results indicate that toluene is a relatively good solvent at low concentration but as the RDF (radial distribution function) never rises above 1 this indicates that at the higher concentrations used for coating OPV devices, polymer−polymer interactions are likely stronger than solvent interactions leading to clustering in toluene. Experimentally, high MW PCDTBT has low solubility in most solvents and is most soluble in di- and trichlorobenzenes, consistent with our solution model.

Figure 8 shows radial distribution functions of the sulfur atoms in the 4 chain simulations. The left figure is the RDF of all sulfurs. The right figure is the RDF of all sulfurs in one chain renormalized to the same peak height. We clearly see some differences. There is a small shoulder at short distances which is more pronounced between different chains which indicates aggregation between chains. The lack reduced size of this peak in the single chain simulation indicates that close interaction within one chain is sterically hindered. Also the shape of the first peak changes and the area at a distance of about 1 nm is higher for multiple chains. Again this shows that structure formation is constrained in this polymer by stiff bonds and long equilibration times caused by low solubility.

IV. CONCLUSION

We carried out the first molecular dynamics simulation of the organic photovoltaic PDCTBT 12-mer in toluene solvent. This simulation provides insight into the atomic scale structure and structural order of the polymer in solution. We found alternating orientation along the backbone or a dihedral angle

dx.doi.org/10.1021/je500101b | J. Chem. Eng. Data 2014, 59, 2982−2986

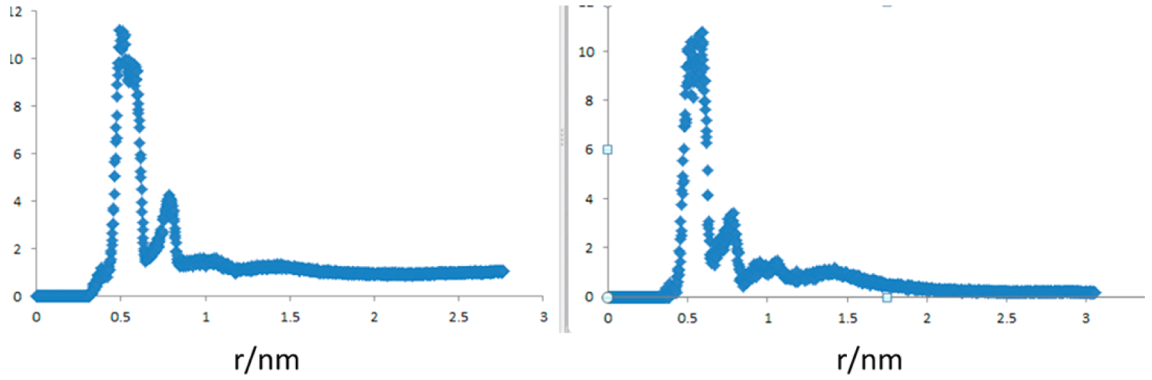

Figure 8. Radial distribution functions between sulfur atoms in the simulation with four polymers (averaged between 2 and 3 ns). Left, all sulfurs; right, all sulfurs along one chain.

distribution centered around 90°, which indicates that the polymer is unconjugated in solution and that a planar configuration in a device is not thermodynamically favored. We suggest that the structural configuration can be improved by hindering the motion of the thiophene molecular rings by adding side groups which lock successive rings through, for example, hydrogen bonding. We also find initial indications of aggregation for multiple chains. This simulation has good correlation with experimental results, as PCDTBT shows poor solubility experimentally and requires significant equilibration time to form optimized structures. In the future, this simulation technique and theoretical technique will help researchers discover new, high-quality materials for power generation. There is, however, always the caveat that the results are only as reliable as the model employed. In this first study we decided to use a simple generic force-field which was not optimized for the problem under study or OPVs in general. Therefore, one has to be cautious in interpreting the data, especially with respect to the conjugations of the system, as in the generation of such a simple model no particular attention was given to correct conjugation. Therefore, further studies with better optimized models are in order.

AUTHOR INFORMATION

Corresponding Author

*E-mail: rfaller@ucdavis.edu.

Notes

The authors declare no competing financial interest.

REFERENCES

(1) Brabec, C. J.; Hauch, J. A.; Schilinsky, P.; Waldauf, C. Production Aspects of Organic Photovoltaics and Commercialization of Devices. *MRS Bull.* **2005**, *30*, 50−52.

(2) Rohr, S. *Heliatek Consolidates Its Technology Leadership by Establishing a New World Record for Organic Solar Technology with a Cell Efficiency of 12%*; Heliatek Company Report; Heliatek: Dresden, Germany, 2013.

(3) Walzer, K.; Maennig, B.; Pfeiffer, M.; Leo, K. Highly Efficient Organic Devices Based on Electrically Doped Transport Layers. *Chem. Rev.* **2007**, *107*, 1233−1271.

(4) Barker, J. A.; Ramsdale, C. M.; Greenham, N. C. Modeling the Current−Voltage Characteristics of Bilayer Polymer Photovoltaic Devices. *Phys. Rev. B* **2003**, *67*, 075205.

(5) Yu, G.; Gao, J.; Hummelen, J. C.; Wudl, F.; Heeger, A. J. Polymer Photovoltaic Cells: Enhanced Efficiencies via a Network of Internal Donor−Acceptor Heterojunctions. *Science* **1995**, *270*, 1789−1791.

(6) Service, R. F. Solar Energy. Outlook Brightens for Plastic Solar Cells. *Science* **2011**, *332* (6027), 293.

(7) Park, S. H.; Roy, A.; Beaupré, S.; Cho, S.; Coates, N.; Moon, J. S.; Moses, D.; Leclerc, M.; Lee, K.; Heeger, A. J. Bulk Heterojunction Solar Cells with Internal Quantum Efficiency Approaching 100%. *Nat. Photonics* **2009**, *3*, 297−302.

(8) Chu, T.-Y.; Alem, S.; Verly, P. G.; Wakim, S.; Lu, J.; Tao, Y.; Beaupré, S.; Leclerc, M.; Bélanger, F.; Désilets, D.; Rodman, S.; Waller, D.; Gaudiana, R. Highly Efficient Polycarbazole-Based Organic Photovoltaic Devices. *Appl. Phys. Lett.* **2009**, *95*, 063304.

(9) Wakim, S.; Beaupré, S.; Blouin, N.; Aich, B.-R.; Rodman, S.; Gaudiana, R.; Tao, Y.; Leclerc, M. Highly Efficient Organic Solar Cells Based on a Poly(2,7-carbazole) Derivative. *J. Mater. Chem.* **2009**, *19*, 5351−5358.

(10) Cho, S.; Seo, J. H.; Park, S. H.; Beaupré, S.; Leclerc, M.; Heeger, A. J. A Thermally Stable Semiconducting Polymer. *Adv. Mater.* **2010**, *22*, 1253−1257.

(11) Chu, T.-Y.; Alem, S.; Tsang, S.-W.; Tse, S.-C.; Wakim, S.; Lu, J.; Dennler, G.; Waller, D.; Gaudiana, R.; Tao, Y. Highly Efficient Polycarbazole-Based Organic Photovoltaic Devices. *Appl. Phys. Lett.* **2011**, *98*, 253301−253301−3.

(12) Beiley, Z. M.; Hoke, E. T.; Noriega, R.; Dacuña, J.; Burkhard, G. F.; Bartelt, J. A.; Salleo, A.; Toney, M. F.; McGehee, M. D. Morphology-Dependent Trap Formation in High Performance Polymer Bulk Heterojunction Solar Cells. *Adv. Energy Mater.* **2011**, *1*, 954−962.

(13) Etzold, F.; Howard, I. A.; Mauer, R.; Meister, M.; Kim, T.-D.; Lee, K.-S.; Baek, N. S.; Laquai, F. Ultrafast Exciton Dissociation Followed by Nongeminate Charge Recombination in PCDTBT:PCBM Photovoltaic Blends. *J. Am. Chem. Soc.* **2011**, *133*, 9469−9479.

(14) Li, Z.; McNeill, C. R. Transient Photocurrent Measurements of PCDTBT:PC70BM and PCPDTBT:PC70BM Solar Cells: Evidence for Charge Trapping in Efficient Polymer/Fullerene Blends. *J. Appl. Phys.* **2011**, *109*, 074513−074517.

(15) Sun, Y.; Takacs, C. J.; Cowan, S. R.; Seo, J. H.; Gong, X.; Roy, A.; Heeger, A. J. Efficient, Air-Stable Bulk Heterojunction Polymer Solar Cells Using MoOx as the Anode Interfacial Layer. *Adv. Mater.* **2011**, *23*, 2226−2230.

(16) Staniec, P. A.; Parnell, A. J.; Dunbar, A. D. F.; Yi, H.; Pearson, A. J.; Wang, T.; Hopkinson, P. E.; Kinane, C.; Dalgliesh, R. M.; Donald, A. M.; et al. The Nanoscale Morphology of a PCDTBT:PCBM Photovoltaic Blend. *Adv. Energy Mater.* **2011**, *1*, 499−504.

(17) Chang, Y.-M.; Zhu, R.; Richard, E.; Chen, C.-C.; Li, G.; Yang, Y. Electrostatic Self-Assembly Conjugated Polyelectrolyte-Surfactant Complex as an Interlayer for High Performance Polymer Solar Cells. *Adv. Funct. Mater.* **2012**, *22*, 3284−3289.

(18) Wang, D. H.; Moon, J. S.; Seifter, J.; Jo, J.; Park, J. H.; Park, O. O.; Heeger, A. J. Sequential Processing: Control of Nanomorphology in Bulk Heterojunction Solar Cells. *Nano Lett.* **2011**, *11*, 3163−3168.

(19) Cowan, S. R.; Leong, W. L.; Banerji, N.; Dennler, G.; Heeger, A. J. Identifying a Threshold Impurity Level for Organic Solar Cells: Enhanced First-Order Recombination via Well-Defined PC84BM

Traps in Organic Bulk Heterojunction Solar Cells. *Adv. Funct. Mater.* **2011**, *21*, 3083−3092.
(20) Etzold, F.; Howard, I. A.; Forler, N.; Cho, D. M.; Meister, M.; Mangold, H.; Shu, J.; Hansen, M. R.; Müllen, K.; Laquai, F. The Effect of Solvent Additives on Morphology and Excited-State Dynamics in PCPDTBT:PCBM Photovoltaic Blends. *J. Am. Chem. Soc.* **2012**, *134*, 10569−10583.
(21) Liu, X.; Huettner, S.; Rong, Z.; Sommer, M.; Friend, R. H. Solvent Additive Control of Morphology and Crystallization in Semiconducting Polymer Blends. *Adv. Mater.* **2012**, *24*, 669−674.
(22) Moon, J. S.; Jo, J.; Heeger, A. J. Nanomorphology of PCDTBT:PC70BM Bulk Heterojunction Solar Cells. *Adv. Energy Mater.* **2012**, *2*, 304−308.
(23) Troisi, A.; Cheung, D.; Andrienko, D. Charge Transport in Semiconductors with Multiscale Conformational Dynamics. *Phys. Rev. Lett.* **2009**, *102*, 18−21.
(24) Madison, T. a.; Gagorik, A. G.; Hutchison, G. R. Transport in Imperfect Organic Field Effect Transistors: Effects of Charge Traps. *J. Phys. Chem. C* **2012**, *116*, 11852−11858.
(25) Hess, B.; van der Spoel, D.; Lindahl, E.; Apol, E.; Apostolov, R.; Berendsen, H. J. C.; van Buuren, A.; Bjelkmar, P.; van Drunen, R.; et al. *GROMACS USER MANUAL 4.5.*; Royal Institute of Technology and Uppsala University: Sweden, 2010; www.gromacs.org.
(26) Wang, J.; Wang, W.; Kollman, P. a; Case, D. a. Automatic Atom Type and Bond Type Perception in Molecular Mechanical Calculations. *J. Mol. Graph. Model.* **2006**, *25*, 247−260.
(27) Wang, J.; Wolf, R. M.; Caldwell, J. W.; Kollman, P. a; Case, D. a. Development and Testing of a General Amber Force Field. *J. Comput. Chem.* **2004**, *25*, 1157−1174.
(28) Amber Tools website. http://ambermd.org/#AmberTools (accessed March 31, 2014).
(29) McCulloch, I.; Heeney, M.; Bailey, C.; Genevicius, K.; Macdonald, I.; Shkunov, M.; Sparrowe, D.; Tierney, S.; Wagner, R.; Zhang, W.; et al. Liquid-Crystalline Semiconducting Polymers with High Charge-Carrier Mobility. *Nat. Mater.* **2006**, *5*, 328−333.